

Shear strength of connections between open and closed steel-concrete composite sandwich structures

Woo-Bum Kim¹ and Byong Jeong Choi^{*2}

¹*Department of Architectural Engineering, Kongju National University, Kongju, Korea*

²*Department of Architectural Engineering, Kyonggi University, Kyonggido, Korea*

(Received April 02, 2010, Accepted February 21, 2011)

Abstract. The behavior of connections between open sandwich slabs and double steel skin composite walls in steel plate-concrete(SC) structure is investigated by a series of experimental programs to identify the roles of components in the transfer of forces. Such connections are supposed to transfer shear by the action of friction on the interface between the steel surface and the concrete surface, as well as the shear resistance of the bottom steel plate attached to the wall. Experimental observation showed that shear transfer in slabs subjected to shear in short spans is explained by direct force transfer via diagonal struts and indirect force transfer via truss actions. Shear resistance at the interface is enhanced by the shear capacity of the shear plate as well as friction caused by the compressive force along the wall plate. Shear friction resistance along the wall plate was deduced from experimental observation. Finally, the appropriate design strength of the connection is proposed for a practical design purpose.

Keywords: Wall-slab connections, steel plate-concrete structure, composite wall, shear plate, SC structure

1. Introduction

The steel plate concrete structure (hereinafter SC structure) is one of the viable options for the reduction of construction duration as well as to enable modular systems in nuclear power plants (AIJ 2005, BSI 2004, Chorus 2004, Han 2002, Kanchi 1996, Liang 2006, Liew *et al.* 2009, Tao 2008, and Uy 2001). The SC structure consists mainly of double steel skin wall and open sandwich composite slab, whereas open sandwich composite slabs serve as gravity-resisting systems. McKinley made a various research on the double skin system area and he addressed the efficient lateral resistance of the double skin research (McKinley 2002). Recently, the structural behavior of SC wall and slab systems under various loading conditions has been studied for the purpose of preparing SC structure specifications for nuclear plant structures in Korea (Kim *et al.*, 2008 and Choi *et al.*, 2009). In this research, the behavior and strength of the connection and axial strength of the SC structure is investigated to formulate design guidelines. The connection in an SC structure is resisted by two components: (1) the friction force between the steel wall and concrete slab; and (2) the shear force of the shear plate. The capacity of each component depends on loading and boundary conditions. Unfortunately, there have been few studies performed on the SC connection so far because of its rare application to common structures except nuclear power plants. For this class of problem, shear friction

* Corresponding author, Professor, E-mail: bjchoi@kyonggi.ac.kr

approach is the preferred method of solution. Practical applications of direct shearing are found in the design of composite concrete beams (Loov *et al.* 1994), corbels (Mattock 1976), and offshore foundation caisson (Walraven *et al.* 1987). Shear design methods based on shear friction model (Birkeland 1966, Mast 1968, Loov 1998, and Hofbeck *et al.* 1969) require determination of the shear strength envelope of concrete material, i.e., the relationship between the mobilized shear stress and the applied normal stress in the failure. The normal confining stress exerted at the sheared section was assumed to be equal to the forces derived from yielding of steel reinforcements. Most of this research focused on shear transfer in concrete by shear friction under direct shearing. However, if shear force is transferred by two components such as steel plate-concrete interface and shear plate, different shear transfer mechanisms are developed according to the loading. No successful mechanical approach to quantify the shear capacity at the interface has been performed because of its complex load distribution behavior. This study focused on the shear strength capacity and rigidity of the connections. To investigate the behavior of the connections, full-scale specimens reflecting the actual design of nuclear power plant structures were made and tested. Friction force and friction coefficient at the interface, shear force of shear plate, and the tensile stress on the top reinforcing were examined. Friction force and shear force developed at the interface were deduced by measuring the strain of the shear plate. The friction coefficient was obtained from the deduced friction force and the compressive force at the interface. Also, the rigidity of the connections had been examined as different rotational capacities were expected unlike in ordinary connections. Finally, the shear strength formula was proposed based on the experimental result and logical explanation.

2. Experimental program

2.1 Specimen description

Four specimens were prepared as shown in Fig. 1 and Table 1, of which two consisted of open steel sandwich slabs and the other two were made of conventional reinforced concrete slabs with seven reinforcing bars in the bottom layer. One of the open sandwich slabs has studs on the steel wall plate with the shear plate welded to the walls by fillet welding. The first stirrup was placed at 280 mm from the support. The 13-mm-diameter head studs were spaced 180 mm apart. Also, one of the reinforced concrete slabs has a shear plate welded to the wall and the other has no shear plate (see Fig. 1(c) and 1(d)). SC slabs are connected to walls through five 25-mm-diameter reinforcing steel bars and 12-mm-thick shear plate at the bottom welded to the wall's steel plate. The wall section was 994 mm thick and 720 mm wide. The reinforcing bars were penetrated through holes of the wall plates. The material properties are summarized in Table 2.

2.2 Test set-up

The slabs between the wall and simple support were subjected to concentrated loads. The reactions of the statically indeterminate structures of specimens in this study were measured by two load cells at loading point and simple support as shown in Fig. 2. The differences between the two reaction forces were equal to the shear force at the connection to walls. Deflections at the loading point and rotation angles between walls and slabs were measured. Strains in shear plates were measured to estimate the partial shear resistance of the shear plate. Strains in the top reinforcing bars were measured to estimate

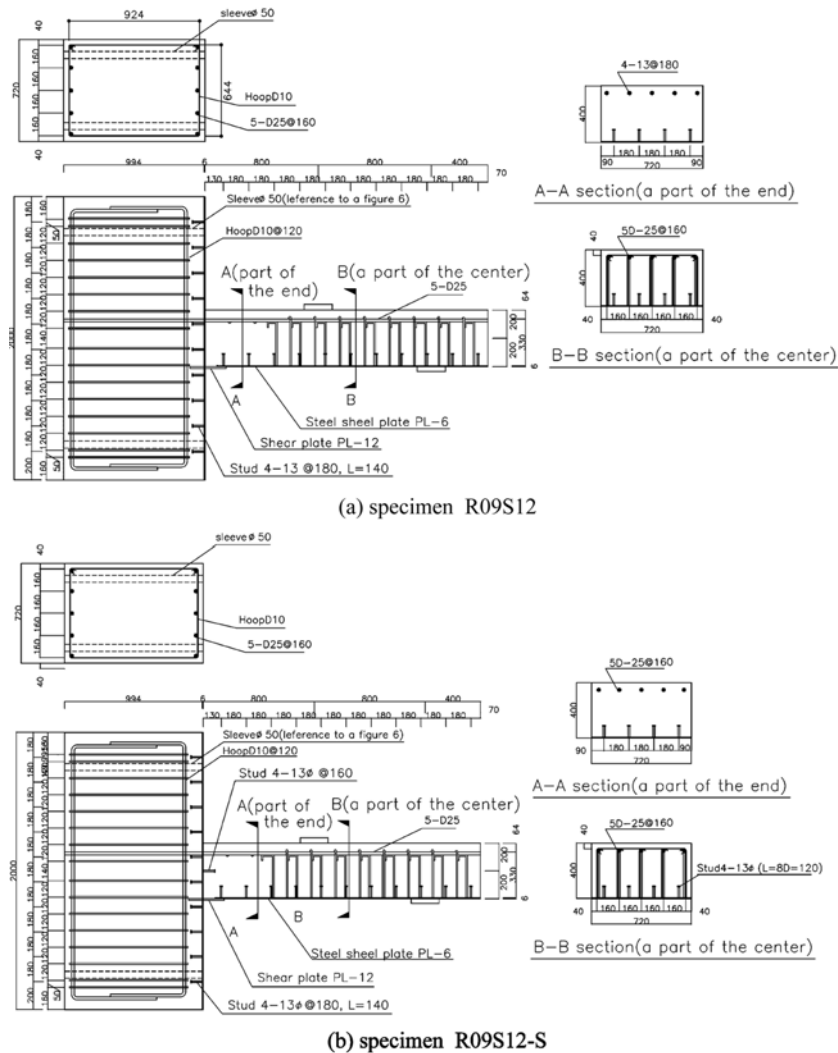


Fig. 1 Test specimen

the pull-out displacement and rotation angle at the interface between the wall and slabs.

The successful connection performance requires an explanation on the clear force transfer between SC walls and slabs. In this study, we investigated shear transfer at the wall to slab and analyzed the joint flexibility. The slab's shear strength itself and the interface were differentiated to clarify the required strength.

3. Experiment results

3.1 Ultimate strength and failure pattern

All of the specimens showed flexural cracking at the beginning of load. As the load approached the ultimate state, shear cracking between the loading point and support were observed as shown in Fig. 3. In case of SC slab specimens, arch cracking formed from the loading point to the shear plate, and this

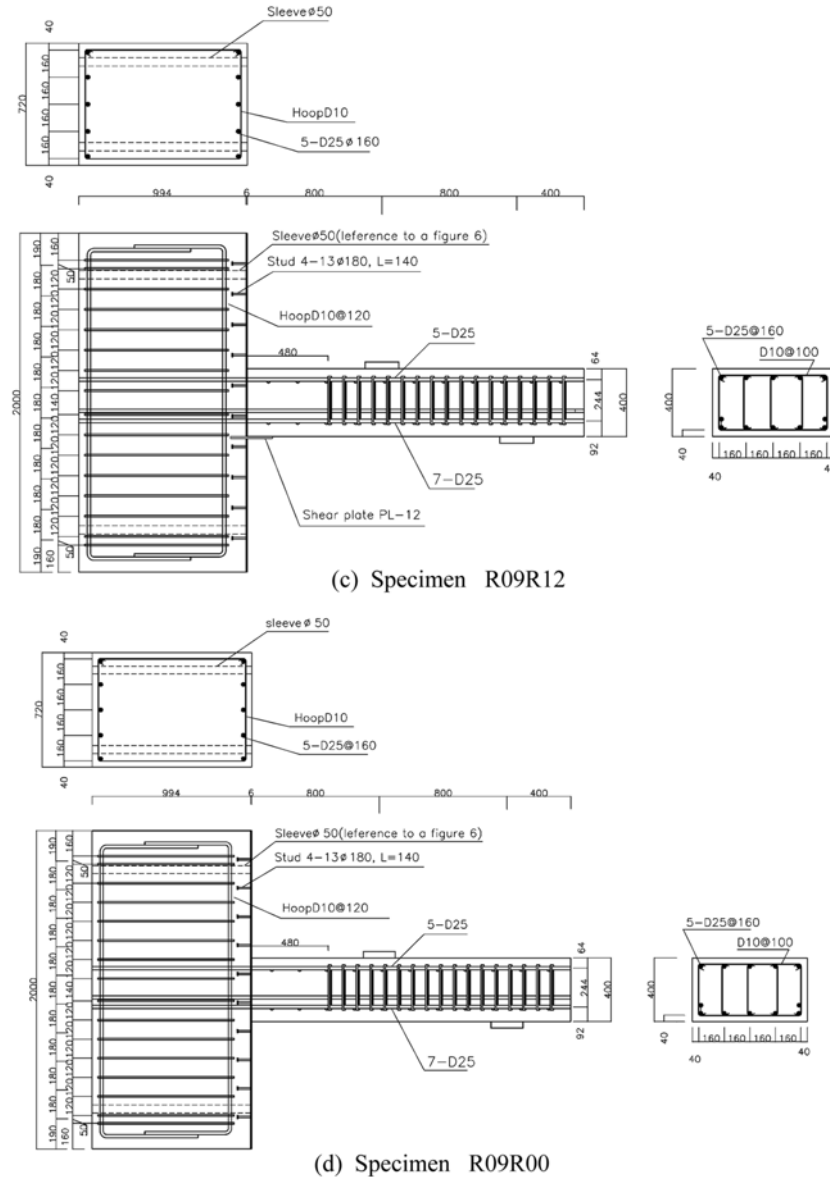


Fig. 1 Continued

resulted in shear failure of the slab. On the other hand, in case of RC slab, a similar arch cracking occurred at the ultimate load, but it formed off the shear plate. The measured maximum applied load and shear force of each specimen are summarized in Table 3.

Shear forces at walls were calculated by the difference between the measured load at the loading point and the measured reaction at the simple support on the right. The deflections at the loading point versus applied force at the loading point are plotted in Fig. 4. Two of the SC specimens with shear plate showed two peak load points. The first peak load point corresponding to slab strength and the second peak load point corresponding to joint strength were obtained. Also, in case of RC slabs, the specimen

Table 1 Test specimen properties

Specimen	R09S12	R09S12-S	R09R12	R09R00
Slab type	SC	SC	RC	RC
Top reinforcing bar	5-D25			
Steel ratio	0.9%			
Shear plate thickness	12 mm			-
Shear stud	-	4-13@180	-	
Slab dimension	480 mm × 720 mm			
Steel plate thickness	6 mm		-	-
Bottom reinforcement	-		7-D25	

Table 2 Material properties

Component	Material Specification	Size	Nominal Strength (MPa)	Test strength (MPa)
Steel Plate	SS400	PL-6	$F_y = 235, F_u = 400$	$F_y = 242, F_u = 411$
		PL-12		$F_y = 304, F_u = 459$
Stud	SS400	φ13 mm	$F_y = 240, F_u = 400$	$F_y = 323$
Concrete			24.0	28.1
Reinforcement	SD350	D13/ D25	$F_y = 350$	$F_y = 385$

R0.9R-12 with shear plate showed two similar peak points. On the other hand, the specimen R0.9R-00 without shear plate showed only one peak point. Any additional load increase was not observed after the peak point. Therefore, we can know that shear plate contributes to the shear resistance of the wall after the ultimate load.

The specimen R0.9S-12S with studs on the wall showed a higher shear strength and more ductile behavior than the specimen without studs. It was confirmed that the strength of the specimens can be enhanced by the shear studs as well as shear plate in the ultimate and post-ultimate states. The shear studs can be used to replace the shear plate due to the convenience in construction. However, this paper did not cover the shear mechanism caused from the shear stud that is taking care of the whole shear force. In this research, member shear failure occurred prior to joint shear failure in all specimens, and then the strength of the specimens was determined by member shear strength. In the ordinary SC connections in nuclear structure, member shear failure or member flexural failure is expected according to shear span ratio of slab. It is considered that joint shear failure is not likely to occur except special loading and boundary condition. Nevertheless, an investigation of the shear transfer mechanism is needed to deduce the joint shear strength from the experimental results.

3.2 Shear resistance of connection

Shear resistance at the interface relies on shear friction along the surface of the wall plate and the flexural strength of the shear plate. As long as there is no gap between the wall plate and concrete slab, a partial contribution to shear strength by friction is effective.

As shown in the deflection curve in Fig. 4, when the applied load first reached the ultimate load, shear failure occurred in the member. After passing the first ultimate load point, the second ultimate load point was obtained by the shear resistance of the shear plate and friction of the wall. Once diagonal

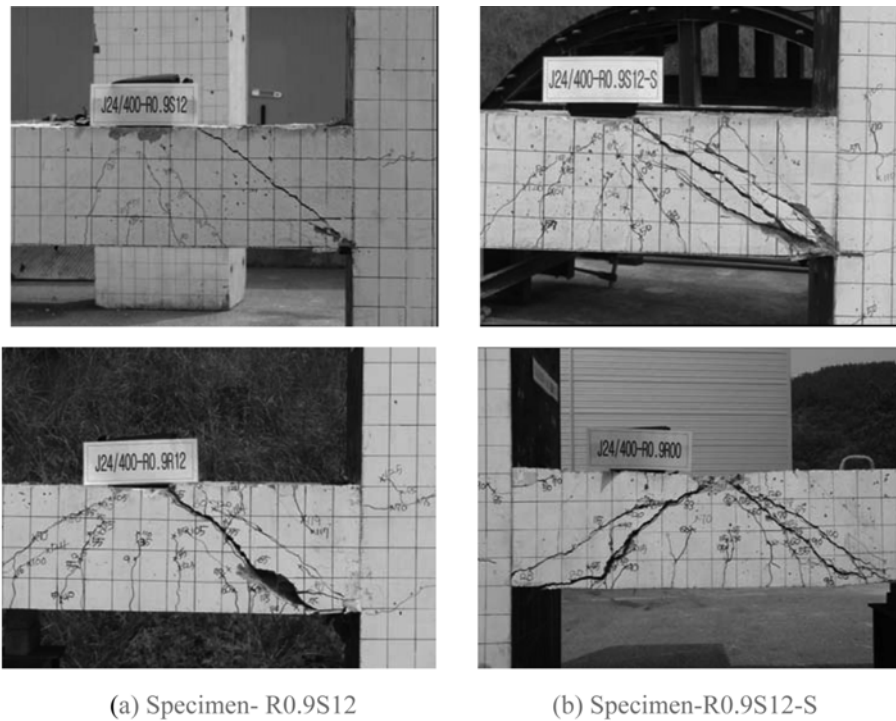


Fig. 3 Crack patterns

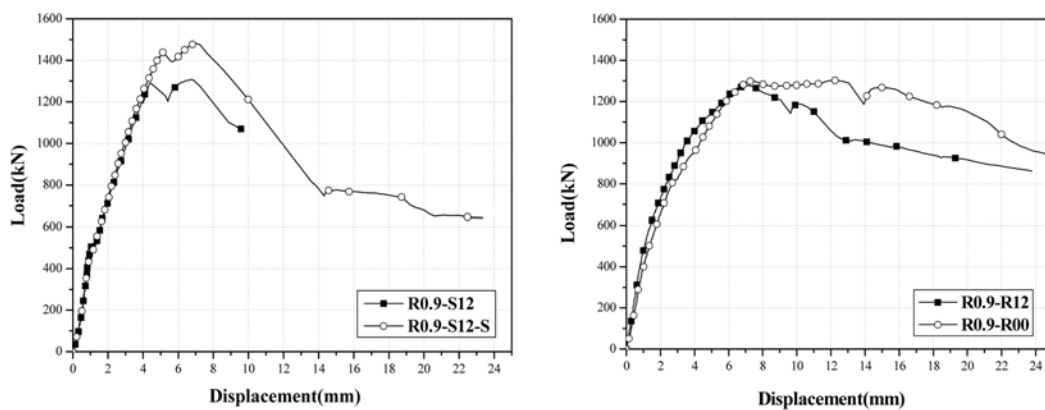


Fig. 4 Load-deflection curves

diagonal cracks developed. However, the ratio increased rapidly to 45%~60% up to the second ultimate load. In other words, the contribution of frictional shear resistance at the interface decreased, and the value was 55%~40% of the total shear force. In the R0.9R12 specimen, the shear force was decreased to account for the weakened shear strength at the load level of 580 kN. This means that the reinforced concrete model does not have the shear plate and it has no more shear strength after the yielding. Thus, simply the numerical negative shear resistance ratio was resulted at the ultimate load level in Fig. 6. On

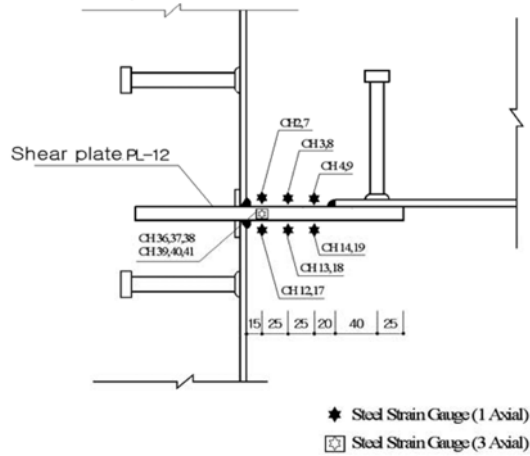


Fig. 5 Measurement of strain in shear plate

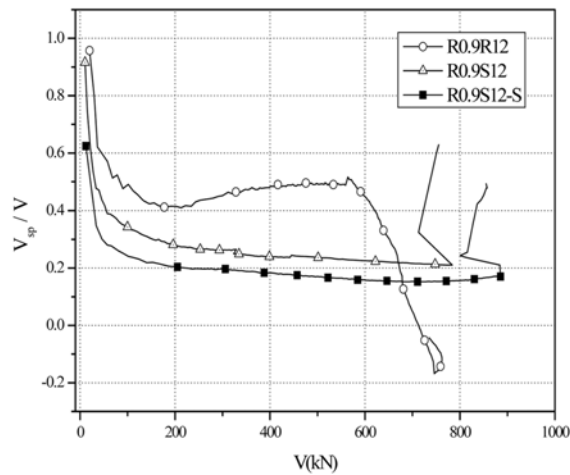


Fig. 6 Ratio of shear resistance by shear plate to total shear

the other hand, in the RC specimen, the ratio decreased after the diagonal crack occurred.

In this case, the shear plate did not transfer the shear force as the crack occurred off the shear plate as previously described. Therefore, it is necessary that shear resistance is allocated to friction surface and shear plate for practical design purpose.

3.2.1 Design shear strength of shear plate

To formulate the proposed design shear strength of the shear plate, the failure mode of the shear plate was investigated. From the strain data of the shear plate obtained in the experiment, it was ascertained that the flexural failure of the shear plate occurred at the second ultimate point. Therefore, we can establish the maximum shear force under the assumption of yielding of the shear plate.

If we assume the triangular load distribution on the shear plate as shown in Fig. 7, the relationship between yield moment and shear force at the shear plate is as follows.

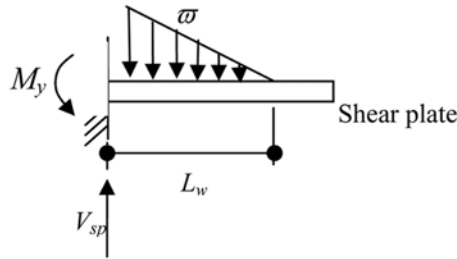


Fig. 7 Assumption of load distribution in shear plate

$$V_{sp} = \frac{3 M_y}{L_w}$$

Here, the value, $L_w=4t$, was obtained empirically in the previous research (Mochida Tetsuo, 1999). By introducing the value of 12 mm of t in case of specimen R09.S12, the shear resistance of the shear plate is 480kN, and this value is close to the 465 kN value ($V_{sp}/V = 0.6$) obtained in the experiment as the final value shown in Fig. 6. The 265 kN value was obtained from the difference between the $V_u (= 758 \text{ kN})$ and $V_{sp}(465 \text{ kN})$ is surmised as friction resistance at the interface.

3.2.2 Design strength of friction at interface

At the interface, friction force, V_{fp} , can be calculated by multiplying the compressive force to friction coefficient between the steel plate of the wall and concrete slab. The compressive force forms as the equal amount of tensile force in the top reinforcing bar. If the applied load reaches the ultimate state and the top reinforced bar reaches its yield point, the friction force is $\mu A_s F_y$. Here, μ is a friction coefficient between the concrete and steel plate and A_s is an area of the top reinforcing bar. In the code ACI 318(ACI 2005), the value of 0.7 for μ is recommended at the surface between concrete and steel. In this experiment, the value of μ ranging from 0.8 to 1.8 was obtained as shown in Fig. 8. But most of the data ranged from 0.8 through 1.2 except the final stages. Here, μ was calculated by dividing $V_{fp}(= V - V_{sp})$ by compressive force, which is equal to the amount of tensile force of the top reinforcing bar. Fig. 9 shows

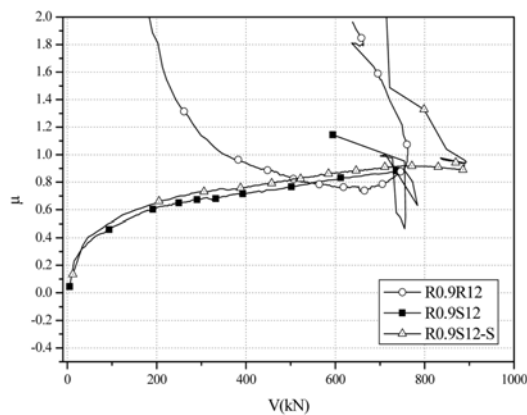


Fig. 8 Friction coefficient

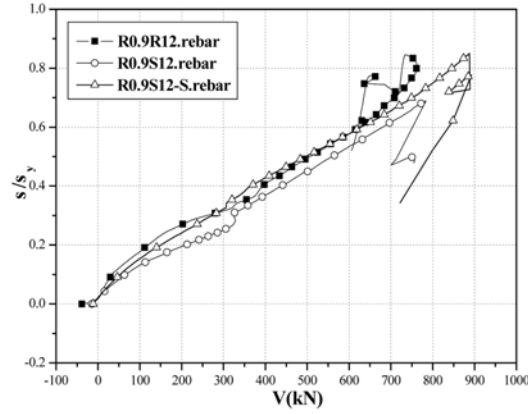


Fig. 9 Stress of top reinforcing bar

the axial stress of the top reinforcing bar and shear plate corresponding to the total shear force at the interface.

The design strength of friction can be expressed in the form of μC . Here, the compressive force, C directly affects the friction strength at the interface. Usually, the compressive force depends on the loading pattern such as location and amount of applied load. Applying the concentrated load adjacently to the interface causes the development of less compressive force because of low end moment. However, in this case, high compressive force can be developed due to direct shear friction effect as described in ACI-318. If we design the connections based on the limit design approach, usually slab design strength is determined in the flexural failure mode. The compressive force will then be $A_s F_y$, which is equal to the tensile force of the top reinforcing bar.

In this research, the stress of the top reinforcing bar was 80% of the yield stress at the ultimate strength as shown in Fig. 9. In this case, the shear span ratio of the slab is about 1.0 and therefore shear failure is dominant. If we design a connection conservatively, the reduction factor Φ can be applied to friction strength with the form of $\Phi \mu A_s F_y$. 1.0 of Φ for the flexure dominant member and 0.5 of Φ for the shear dominant member is recommended based on the test results. Therefore, in this research using the analytical investigation, the design shear strength of the interface is cautiously suggested as follows.

$$V_n = V_{sp} + V_{fr,sp} = 3M_y/L_w + \phi \mu A_s F_y$$

The proposed design strength is compared with experimental shear strength in Table 4. The proposed strength shows 16%~30% lower value than the experimental strength. Then, the design strength can be

Table 4 Proposed design shear strength and experimental shear strength

Specimen	Proposed design strength			Experimental shear strength
	$V_{sp} = 3M_y / L_w + V_{stud}$	$V_f = \phi \mu A_s F_y$	$V_{prop} = V_{sp} + V_{fr}$	V_{exp}
R0.9-S12	330	309	639	757
R0.9-S12-S	431	309	740	890
R0.9-R12	330	309	639	755
R0.9-R00	0	309	309	760

used conservatively in practical design of SC connection.

3.3 Joint rigidity

Concrete discontinuity along the wall plate results in low connection rigidity. Joint rigidity influences the slab's deflection. Therefore, it is necessary to investigate the pull-out displacement as well as the developed moment at the interface. Fig. 10(a) shows the pull-out displacement (δ_{slip}) vs. stress of the top reinforcing bar. The measured pull-out displacement increases up to 0.6-0.65 mm in the SC at steel stress equal to 200 MPa. End moment (M_A) and end rotation (θ_A) at the interface was calculated by using pull-out displacement and pull-out force of the reinforcing bar. End rotation by slip at the interfaces results in lower end moment than fixed end moment. The reduced M_A divided by the fixed end moment M_{FEM} is defined as the degree of fixity k at the connection. Fig. 10(b) shows that rotational stiffness K ($= M_A/\theta_A$) of SC specimens approaches a constant value after 100 MPa of reinforcing steel stress. As shown in Fig. 11, the degree of fixity for the specimens ranged from 0.4 to 0.6, and this value was close to the value calculated from the measured applied load and reaction in Table 3. Using slope deflection equation, the rotational stiffness K at the interface and flexural stiffness EI of slabs is related by k . This assumes that the wall is rigid and the wall plate does not deflect for the elastic application only.

$$k = \frac{Kl}{3EI + Kl}$$

The displacement at loading point is calculated by the following equation in terms of k and K with the effective flexural stiffness of slabs. The effective stiffness considers the cracked section of concrete after flexural cracking. The deflection at the loading point is expressed as

$$\delta_c = \frac{Pl^3}{48EI} \left(1 - \frac{9}{16}k \right)$$

The deflection obtained from the above equation was close to the experimental result as shown in Fig. 12.

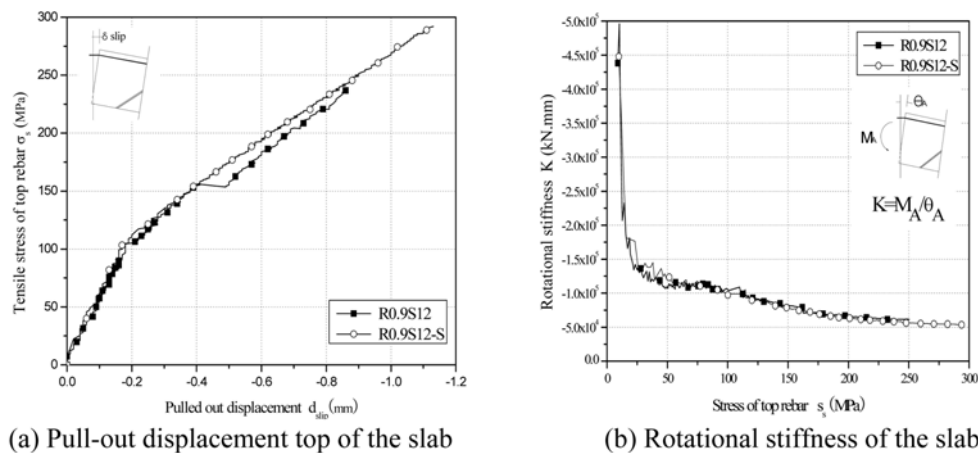


Fig. 10 Rotation of slabs

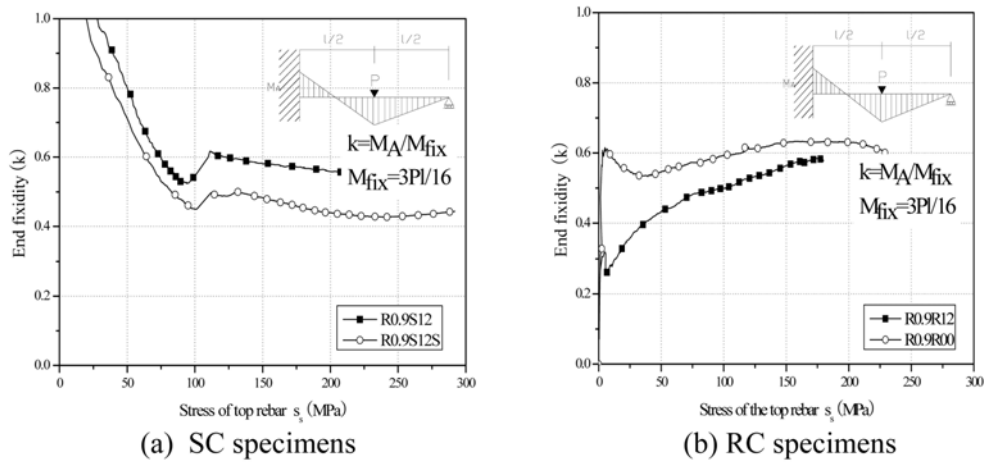


Fig. 11 Rigidity of connections

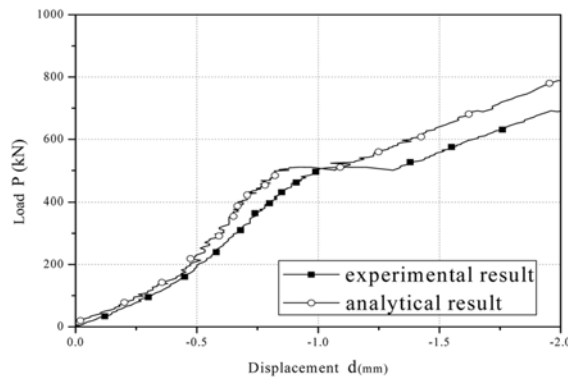


Fig. 12 Comparison of load deflection curve

4. Conclusions

Based on the experimental program of SC slabs, the following conclusion can be drawn:

1. In ordinary wall–slab systems of nuclear plant structures, if the slab’s shear span ratio is larger than 1.0 as in the test specimens in this specific case study, member shear or flexural failure rather than joint failure is expected to occur. When member shear failure occurs prior to joint shear failure, a different shear transfer was observed after diagonal member cracking, and the contribution of the shear plate in shear resistance increased.

2. Measured friction coefficients at the interface between the steel and concrete surface ranged from 0.8 to 1.8 and these values were larger than the 0.7 specified in ACI 318.

3. Joint shear design strength considering the capacity of shear plate and friction surface is proposed based on the experimental observation. In calculation of joint strength, 0.5 of Φ for the shear dominant member, and 1.0 for the flexure dominant member can be used for conservative design purposes.

4. Joint rigidity was investigated by measuring end moment and rotation. The degree of rigidity ranged from 0.4 to 0.6. The deflection of the slab considering the effect of joint rigidity was calculated

by using the slope deflection equation and experimental data.

Acknowledgement

This research is sponsored by the project “Modularization of Nuclear Power Plant Construction” in the Electric Power Industry Technology Evaluation and Planning (ETEP) in 2008.

References

- ACI-318-05(2005), Building Requirements for Structural Concrete, ACI.
- AII, Architectural Institute of Japan (2005), Seismic Design guideline for Double Steel Skin Wall Systems JEAG 4618.
- Birkeland, P.W. and Birkeland, H.W. (1966), “Connections in precast concrete construction,” *J. American. Concr. Inst.*, **63(3)**, 345-368.
- BSI, British Standards Institution (2004), Eurocode 4, “Design of composite steel and concrete structures”, Part 1.1: General rules for building, DD-0ENV 1994-1-1, London.
- Choi, Byong Jeong. *et al* (2009), “An experiment on compressive profile of the unstiffened steel plate concrete structures under compression loading,” *Steel. Comp. Struct.*, December 1. **9(9)**, 519-534.
- Chorus (2004), “An introduction to the corefast system,” Bi-steel Manual.
- Kim, H. K, Kim, Woo Bum, and Kim, Wonki (1998), “Behavior of strength of wall slab connection in SC structures,” *J. Kor. Steel. Struct. Const.*, **20(2)**, P347.
- Kanchi, M. el al. (1996), “Experimental study on a concrete filled steel structures,” Part 2., Compressive test, *Architectural Ins. Japan. Conf.*, 1071-1072.
- Liew, J.Y.R and Sohel, K.M.A (2009), “Light weight steel-concrete-sandwich system with J-hook connectors”, *Eng. Struct.*, **31(5)**, 1166-1178.
- Loov, R.E. and Patnaik, A.K. (1994), “Horizontal shear strength of composite concrete beams with a rough interface,” *PCI Journal*, **39(1)**, 48-65.
- Mast, R.F. (1968), “Auxiliary reinforcement in concrete connections,” *J. Struct. Div.*, ASCE 94 (ST6) 1485-1504.
- Mattock, A.H. (1976), “Design proposals for reinforced concrete corbels,” *PCI Journal*, **25(3)** 18-25.
- McKinley, B. and Boswell, L.F.(2002): “Behavior of double skin composite construction,” *J. Const. Steel. Res.*, **58**.
- Mochida Tetsuo(1999), “Experimental study on the steel plate reinforced concrete structure part 38 shear transfer mechanism of wall-salab connection,” Proceedings of Architectural Institute of Japan, September.
- Liang, Q.Q, Uy, B. and Richard Liew, J.Y.(2006), “Nonlinear modeling and evaluation of concrete-filled steel stubular columns with local buckling effects,” *J. Constr: Steel. Res.* **62(6)**, 581-591.
- Loov R.E. (1998), “Review of A23.3-94 simplified method of shear design and comparison with results using shear friction,” *Canadian. J. Civil. Eng.*, **25**, 437-450.
- Han, L.H. (2002), “Tests on stub columns of concret-filled RHS sections,” *J. Constr: Steel. Res.*, **58(3)**, 353-372.
- Hofbeck, J.A.,Ibrahim, I.O. and Mattock A.H. (1969), “Shear transfer in reinforced concrete,” *J. American. Con. Ins.*, **66(2)**, 119-128.
- Tao, Z., Han, L.H. and Wang, D.Y (2008), “Strength and ductility of stiffened thin-walled hollow steel structural stub columns filled with concrete,” *Thin-Wall. Struct.*, **46(10)**, 1113-1128.
- Uy, B. (2001), “Strength of short concrete filled high strength steel box columns,” *J. Constr: Steel. Res.*, **57(2)**, 113-134.
- Walraven, J.C., Frenay, J., and Pruijssers, A. (1987), “Influence of concrete strength and load history on the shear friction capacity of concrete members,” *PCI Journal*, **32(1)**, 66-84.